CAVITATION INCEPTION IN SPOOL VALVES

C. S. Martin, Professor
H. Medlarz, Graduate Research Assistant
School of Civil Engineering
Georgia Institute of Technology
Atlanta, Georgia

D. C. Wiggert, Associate Professor
Department of Civil Engineering
Michigan State University
East Lansing, Michigan

C. Brennen, Associate Professor
Department of Mechanical Engineering
California Institute of Technology
Pasadena, California

ABSTRACT

Cavitation has been investigated in directional control valves in order to identify damage mechanisms characteristic of components of aircraft hydraulic systems. Tests have been conducted in a representative metal spool valve and in a model three times larger. Data taken under non-cavitating conditions with both valves showed that the position of the high-velocity annular jet shifts orientation depending upon valve opening and Reynolds number. By means of high-frequency response pressure transducers strategically placed in the valve chamber cavitation could be sensed by the correlation of noise with a cavitation index. The onset of cavitation can be detected by comparing energy spectra for a fixed valve opening and a constant discharge. Another sensitive indicator of cavitation inception is the ratio of cavitating to non-cavitating spectral densities. The incipient cavitation number as defined in this investigation is correlated with the Reynolds number for both valves.

NOMENCLATURE

A	= area of annular orifice
A_c	= area of vena contracta
a	= acoustic velocity
B_1, B_2, B_3	= coefficients
C_c	= coefficient of contraction
C_d	= coefficient of discharge
c	= radial distance between spool and wall
D	= spool diameter
d	= radial distance between spool neck and valve body
e	= radial eccentricity between spool and valve body
f	= frequency
K	= coefficient
ℓ	= axial distance along jet centerline
p	= pressure
p'	= fluctuating pressure
p_1	= pressure at transducer P_1
p_2	= pressure at transducer P_2
p_c	= mean pressure in chamber
p_L	= load (upstream) pressure
p_R	= return (downstream) pressure
p_v	= vapor pressure
$R = Q/\pi D\nu$	= Reynolds number
t	= time
u'_o	= fluctuating velocity on jet
V_c	= velocity in vena contracta
V_j	= jet velocity
V_o	= approach velocity
x	= axial position of valve spool
$\ddot{x}$	= acceleration of spool
Δf	= width of frequency channel
$\Delta p = p_L - p_R$	= pressure differential across valve
μ	= dynamic viscosity of liquid
ν	= kinematic viscosity of liquid
ρ	= mass density of liquid
$\sigma = p_c - p_v/\Delta p$	= cavitation index

INTRODUCTION

Cavitation is not nearly as well documented in oil hydraulic systems as it is in such water hydraulic systems as pumps, propellers, hydraulic turbines, and hydrofoils. In aircraft hydraulic systems cavitation most frequently occurs in system valves, pumps, and actuators. Large differences in pressure is a frequent cause of small-scale cavitation in chambers of four-way spool valves, while high frequency motion of a valve-controlled actuator can lead to large-scale cavitation in the cylinder. Another source of cavitation in aircraft hydraulic systems is the improper filling of the pistons on an axial-piston pump. Either during transient loading or under steady-state operation cavitation can occur in the return chamber of directional control valves because of the large pressure drop across the orifice. It is of interest to know the potential cavitation damage as well as any effect of cavitation on system performance under both steady and unsteady flow conditions. Criteria should be established for the onset of cavitation, and damage mechanisms need be identified once cavitation is extensive.

The amount of literature on cavitation in oil hydraulic components is rather sparse. The major publications in the English language are referred to in the book by McCloy and Martin [1]. There is also important literature in German, principally from the fluid power group at the Technical University of Aachen. Cavitation was investigated to a limited extent by MacLellan et al [2] in their laboratory study in an enlarged two-dimensional model of a piston-type control valve. Later but more complete work on cavitation in spool valves was reported by McCloy and Beck [3], who established criteria for cavitation

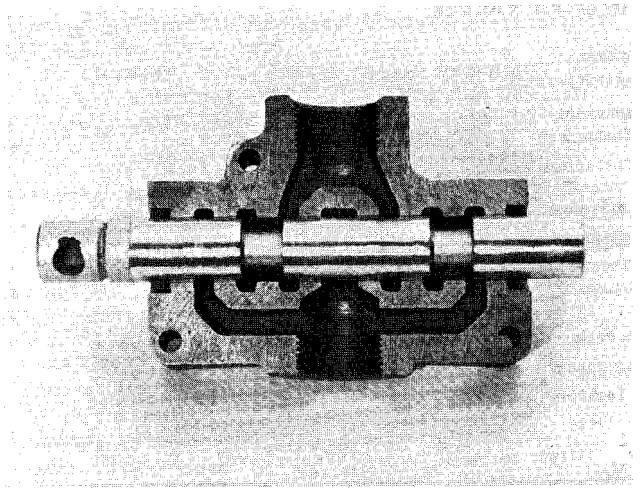

Fig. 1 Spool and cutaway of prototype valve

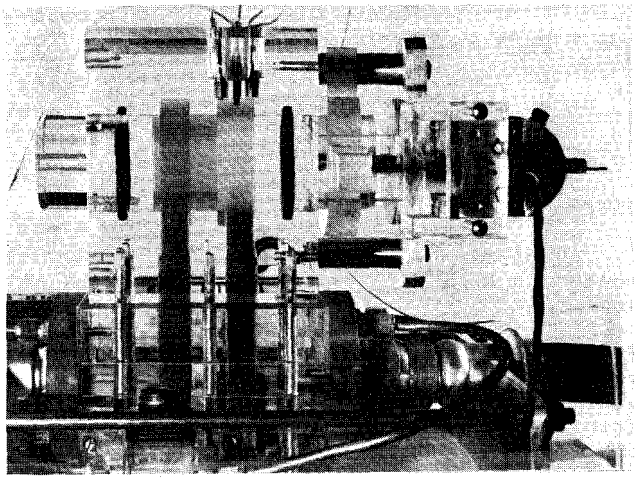

Fig. 2 Side view of model valve

inception in two valves, both two dimensional, one with water and the other with oil as the test liquid. Backé and Benning [4], Backé and Riedel [5], and Riedel [6] all report on cavitation in short orifices using hydraulic oil. The effect of gas content and orifice length on desinent and incipient cavitation is reported by Lichtarowicz and Pearce [7]. Flow pattern changes under both non-cavitating and cavitating flow conditions were documented by McCloy and Beck [8].

An experimental investigation was undertaken to study cavitation damage mechanisms in aircraft hydraulic systems. The purpose of the investigation was to identify mechanisms which lead to damage. A test facility was designed which allowed for the measurement of hydraulic parameters under both non-cavitating and cavitating conditions. Diagnostic techniques were developed to detect the onset and the extent of cavitation. Cavitation inception, its definition and the formation of criteria, are the subject of this paper.

TEST FACILITY

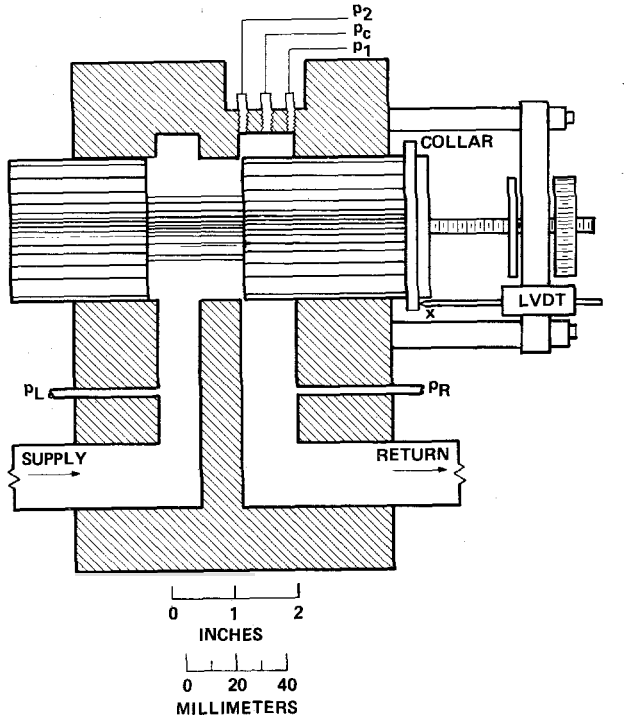

Fig. 3 Longitudinal section of model valve

Cavitation has been investigated in directional control valves in order to identify damage mechanisms characteristic of components of aircraft hydraulic systems. Tests have been conducted in both a metal prototype valve and a plexiglass model three times its size. A common test facility was designed that allowed for control of flow, upstream pressure, downstream pressure, dissolved gas content, and spool position. In order to facilitate the continuous positioning of the spool as well as the mounting of instrumentation on the spool itself, a simple industrial four-way lever-operated spool valve was chosen as the prototype. A cutaway of this valve, which has a spool diameter of 19.05 mm (0.75 in), is shown in Fig. 1. In order to maximize the pressure differential across the valve, only one half of the valve was used, resulting in effect a two-way valve.

A photograph of the plexiglass model, which had a spool diameter of 57.2 mm (2.25 in) is shown in Fig. 2. The size of the valve chamber, lands, and ports of the model valve were scaled up from the metal prototype valve. Fig. 3 is a longitudinal view of the body of the model valve. The opening of the annular space could be controlled by the mechanism attached to the end of the spool. A similar mechanism was installed on the end of the prototype valve. The supply and return ports in the vicinity of the model spool were made to scale with the prototype valve.

The common hydraulic test loop consisted of a 75-hp axial piston pump with a pressure regulator, a high pressure supply line, a flow meter, a bypass system, the particular test valve and its instrumentation, downstream valves for back pressure control, and

a low pressure return line to the pump. The pump had a maximum flow capacity of 0.0025 cms (40 gpm) and a maximum supply pressure of 34.5 MPa (5000 psi). Most data were taken with supply pressures less than 18.6 MPa (2700 psi) and flow rates less than 0.00189 cms (30 gpm). The supply pressure to the model was always maintained less than 3.45 MPa (500 psi). A high pressure filter with an absolute rating of 3μm was in continuous use for control of contaminants.

An auxiliary system consisting of a vacuum tank, tubing and valves, and a rubber bag storage reservoir was used to degas the oil. Oil was pumped from the closed bag through a nozzle on top of the vacuum tank and allowed to film down the sides of the tank. The dissolved air content was monitored by use of an Aerometer, a commercial device similar to a Van Slyke apparatus, which uses a filming technique to remove the gas. At room temperature and atmospheric pressure the dissolved gas content of the oil employed in this investigation varied between 9.5 and 10 percent by volume. The minimum value achieved after several hours of degassing was 4 percent.

For the entire investigation a petroleum-based hydraulic oil (MIL 5606C) was employed as the test liquid. A brief listing of some of the pertinent characteristics of this particular oil are:

Temperature (^{o}C)	Specific Gravity	Viscosity (cS)	Vapor Pressure (mm Hg abs)
20	0.872	29.5	11.6
40	0.857	16.8	25.0
60	0.843	10.4	53.0

INSTRUMENTATION

Flow Rate And Temperature

For the steady flow results reported here mean flow rates and pressures were measured to characterize the test conditions, while dynamic pressures and acceleration were monitored to assess the onset and extent of cavitation. For both test valves a drag type flow meter, Ramapo Model V-1-SB, was used to measure the flow rate. This instrument consists of a circular target mounted on the end of a cantilever beam, which has strain gages attached to it. Targets with ranges of 1-10 gpm and 4-40 gpm were installed, depending upon the sensitivity desired. A 5-volt DC power supply was employed for excitation. The output signal was then amplified by means of a Neff Model 122-222 amplifier. Each target was calibrated in place gravimetrically. An Edison resistance temperature detector and a Fluke Model 8000A multimeter were used to monitor the oil temperature immediately upstream of the test valve in question.

Valve Position

An accurate determination of the position of the specific valve was essential because of the relative small openings in practice. For each valve a linear variable displacement transducer (LVDT) was used to measure the relative position x of the spool. Each LVDT, which was excited by a 6-volt DC supply, was calibrated by means of accurate dial gages and a sensitive voltmeter.

Mean Pressures

Pressure transducers were used to measure mean upstream (load--p_L), differential (Δp), chamber (p_C), and downstream (return--p_R) pressures. Fig. 3 shows the location of the pressure taps for the model valve. In this case the differential pressure is defined by $p_L - p_R$. For the model the load pressure p_L was not measured directly.

The load, return, and differential pressure were measured by either Sensotec Model A5 strain-gage or Pace Models KP15 or P3D variable reluctance diaphragm pressure transducers. The mean chamber pressure p_C for each valve was sensed by Kulite Model XTMS semiconductor pressure transducers. As shown in Fig. 3 transducer P_C is located exactly in the middle of the model chamber. For the prototype valve the chamber transducer is located somewhat downstream of the center of the port.

For all mean pressure transducers the power supply and signal conditioning were furnished by Hewlett-Packard Model 8805A carrier amplifiers, which provided an excitation frequency of 2400 Hz. Each transducer and amplifier assembly was calibrated by means of a dead weight tester.

Dynamic Pressures

Fluctuating pressures in the chamber of each valve were measured for the detection of cavitation by high-frequency response piezoelectric pressure transducers, PCB Model 105 A12. These transducers were flush mounted in the chamber of each valve, as shown in Fig. 3 for the model valve. The diameter of the sensing surface is 2.51 mm (0.099 in). The transducers had a resonant frequency in air of 250 kHz and a nominal sensitivity of 5 mV/psi.

The larger size model allowed for the installation of two PCB transducers, referred to as P_1 and P_2 on Fig. 3. The single piezoelectric transducer in the prototype valve chamber is called P_1. This transducer is located somewhat downstream of the middle of the chamber.

Accelerometer

For the expected detection of mechanical effects in the spool related to cavitation a high-frequency response quartz accelerometer was mounted on the end of the spool of the prototype valve. The miniature accelerometer is a MB Model 306 with an undamped natural frequency of 120 kHz and a sensitivity of 7.64 mV/g.

DATA ACQUISITION SYSTEM

The data acquisition system used to sample the so-called mean signals will be described with reference to Fig. 4. The test valve shown in the illustration could either be the model of the prototype valve. For the model valve there was no measurement of load pressure p_L, nor any accelerometer signal $\ddot{x}$. On the other hand for the prototype valve usually only one piezoelectric pressure transducer (P_1) was used.

Mean Quantities

The central device regarding the collection of mean quantities to characterize the

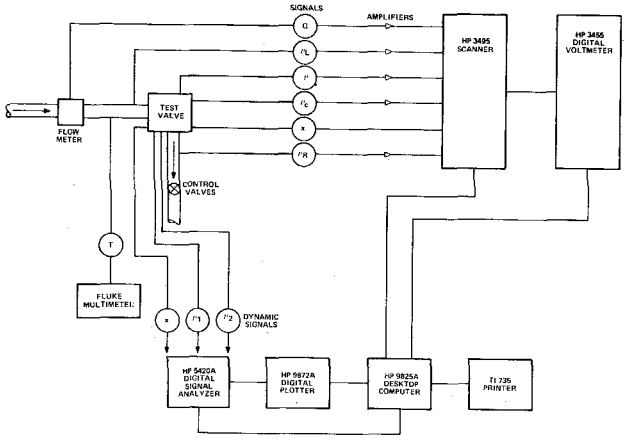

Fig. 4 Data acquisition system

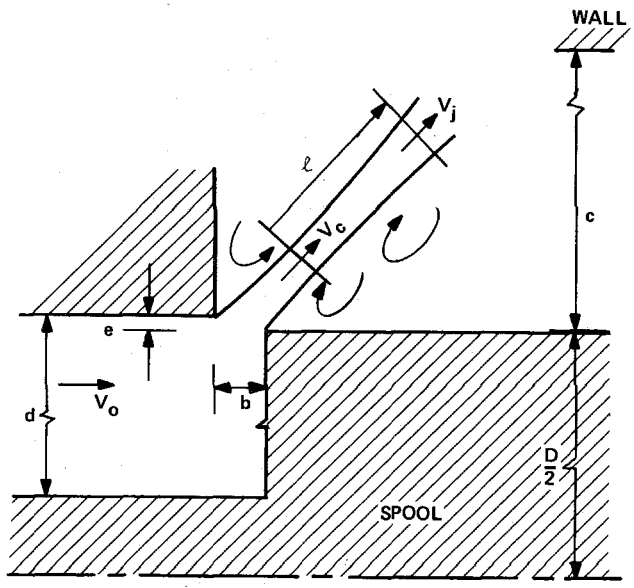

Fig. 5 Definition of valve and jet characteristics

flow conditions is the HP Model 9825A Desktop Computer. This computer controlled the HP Model 3495 Scanner and the HP Model 3455 Digital Voltmeter, both of which are programmable. The analog signal from any of the six input channels shown in Fig. 4 could be transferred through the multiplexer by the controller to the 6-1/2 digit voltmeter, which digitized the signal and transferred the data to the computer. For a given channel twenty samples were averaged to obtain a mean value. The voltages were converted to engineering units by calibration constants which were either input into the computer or retrieved from memory. The resistance output of the Fluke multimeter was keyed into the computer for the computation of temperature. Once the six input channels were scanned and the values computed, the results were transmitted by an interface bus to a TI Model 735 terminal, which was used as a printer. For each flow rate or test condition all of the mean quantities which were printed out could be maintained in the memory of the computer, or discarded. At the completion of the entire test series the data were then stored on a cassette tape of the desktop computer for future retrieval and analysis.

The four-color HP Model 9872A Digital Plotter, which could be controlled by the 9825A Desktop Computer, was utilized for the correlation of data. As mentioned later the plotter could also be controlled by the HP 5420A Signal Analyzer for the plotting of energy spectra.

Dynamic Quantities

As illustrated on Fig. 4 the dynamic quantities monitored in this investigation are the fluctuating pressures p_1 and p_2 and the fluctuating spool acceleration $\ddot{x}$. Any two of these signals could be simultaneously input into the HP 5420A Digital Signal Analyzer, which is an all digital instrument capable of providing both time and frequency domain analysis of complex analog signals in the range of DC to 25.6 kHz. In the time domain the analyzer offers such measurements as time record averaging, probability density function, and auto and cross correlation functions. The various measurement tools available in the frequency domain are linear spectrum, auto and cross spectra, transfer function and coherence function. The calibration constants for the particular instrument could be keyed into the analyzer for direct calculation and display in the appropriate engineering units. The frequency bandwidth could be chosen for the particular application. The analyzer has the capability of instant viewing of both channels on a CRT, and storage of results if desired on a tape cassette, as well as being able to be controlled by the desktop computer. The user can preselect the type of time series analysis most conducive for the specific study -- either sinusoidal, random, or transient. The results could be plotted on the plotter shown in Fig. 4.

Only auto power spectra of the pressure transducer and accelerometer signals are reported here as they proved to be the most meaningful with regard to the detection of cavitation. All data reported were collected with the maximum frequency bandwidth available -- 0 to 25.6 kHz.

VALVE CHARACTERISTICS

The mean flow characteristics of each valve were determined by direct measurement before embarking upon the main cavitation study. It was essential to know accurately the value of the discharge coefficient of the valve in question because of the difficulty in measuring the valve opening with the desired precision. Once the value of the discharge coefficient was known for the particular test conditions the valve opening could then be calculated from the known flow rate and pressure difference across the valve, both of which could be measured quite accurately.

Free streamline theory is applied to the

annular jet issuing from the orifice shown in Fig. 5. Assuming inviscid flow from the approach region

$$\rho \frac{V_o^2}{2} + p_L = \frac{\rho V_c^2}{2} + p_c \quad (1)$$

in which ρ is the fluid density, V_o is the approach velocity, and V_c is the jet velocity in the vena contracta. For the test program considered here the opening b is much less than the annular dimension d, resulting in

$$V_c = \sqrt{\frac{2\Delta p}{\rho}} \quad (2)$$

where $\Delta p = p_L - p_R$, the nominal pressure difference measured by the differential pressure transducer. The volumetric flow rate through the valve

$$Q = A_c V_c \quad (3)$$

in which A_c is the area of the contracted jet, which is usually defined in terms of the area of the annular orifice, or

$$A_c = C_c A = C_c \pi D b \quad (4)$$

in which C_c is the contraction coefficient and D is the diameter of the spool. The resulting relationship for the flow rate is

$$Q = C_d \pi D b \sqrt{\frac{2\Delta p}{\rho}} \quad (5)$$

in which C_d is the discharge coefficient, which in the case for which b<<d, is equal to C_c. The above equation suggests a linear relationship between Q and b.

Because of the relatively small values of b employed in this study and the inherent difficulty in maintaining the desired accuracy in the measurement of b directly for a fixed opening, tests were instead conducted by varying b while holding Δp constant. In this instance the coefficient of discharge could be computed from

$$C_d = \frac{dQ/dx}{\pi D \sqrt{\frac{2\Delta p}{\rho}}} \quad (6)$$

in which x is the axial position of the spool, as measured by the LVDT. Tests conducted at a constant Δp and varying x yielded a linear relationship between Q and x, allowing for the determination of C_d from the slope of the curve.

In general it would be expected that C_d would be a function of the Reynolds number and a cavitation index. For simplicity the Reynolds number is defined on the basis of the average velocity at the annular opening instead of in terms of V_c at the vena contracta. The length dimension chosen in the definition is b, yielding

$$R = \frac{\rho (Q/A) b}{\mu} = \frac{Q}{\pi D \nu} \quad (7)$$

in which μ and ν are the dynamic and kinematic viscosities of the liquid, respectively. For a given temperature Eq. 7 suggests that the Reynolds number is independent of the valve opening b at a constant discharge.

The cavitation index is normally defined as the ratio of a reference pressure minus the vapor pressure of the liquid to a dynamic pressure, the latter of which is referenced to the approach velocity V_o. A more appropriate dynamic pressure for the spool valve would be that based on the jet velocity V_j which is not measured directly, but instead directly related to Δp. The cavitation number is defined as

$$\sigma = \frac{p_c - p_v}{\Delta p} \quad (8)$$

In general it would be expected that the discharge coefficient would depend upon both R and σ, or

$$C_d = C_d(R, \sigma) \quad (9)$$

Extensive testing over a range of R from 150 to 1500 under non-cavitating conditions showed that C_d was independent of viscous effects, yielding an average value of C_d equal to 0.68 for the prototype valve, and 0.66 for the model valve. These values correspond closely to the theoretical value of 0.677 calculated by von Mises using two-dimensional inviscid theory. A summary of the theory is reported by Robertson [9]. Experimental results published by Beck and McCloy [3] show a similar trend. Apparently the Reynolds number defined by Eq. 7 must be less than approximately 100 before viscous effects commence to influence the mean flow characteristics of the valve.

As shown by a number of researchers in the study of cavitation in pipe orifices, cavitation has to become quite extensive before there is any effect on C_d. For the non-cavitating and moderate cavitation reported in this paper it will suffice to use the constant values of 0.68 and 0.66 in any calculations of b from Eq. 5.

TEST PROCEDURE

Once the mean flow characteristics of each valve were determined a test program was initiated to assess both cavitation inception and developed cavitation. The principal instruments used in detecting and defining cavitation were the two transducers P_1 and P_2 for the model valve and transducer P_1 and the accelerometer for the prototype valve. Most of the individual tests were conducted for a constant discharge Q with the spool locked in a fixed position x. Cavitation at various degrees could be established by controlling both the upstream pressure regulator and the downstream ball and needle valves. Once the mean quantities as indicated by the desktop computer corresponded to the desired flow, valve position, and back pressure, the dynamic signals were fed into the signal analyzer.

Although occasionally the cross spectrum and coherence between P_1 and P_2 for the model or P_1 and $\ddot{x}$ for the prototype valve were

measured, the most frequent and useful measurements were the auto power spectra for the two channels. The frequency resolution or Δf for the analysis was 1/256 of the bandwidth, or 100 Hz. By choosing the random option the signals were analyzed using a modified Hanning-type window. The power spectral density function for the auto spectra will be in units of $\sqrt{p'^2}/\Delta f$ for the pressure transducers and $[\overline{d^2x'/dt^2}^2]^{\frac{1}{2}}/\Delta f$ for the accelerometer. By means of cursors the total energy over any frequency range could be quickly extracted from the analyzer, facilitating the real-time analysis and the establishment of criteria for cavitation inception.

NON-CAVITATING SPECTRA

Prior to the establishment of criteria for the inception of cavitation the level of fluctuations of pressure and acceleration had to be understood for non-cavitating flow in each valve. Extensive testing was conducted to correlate energy levels of pressure fluctuations with flow rate and valve opening. Care was taken to insure that the chamber pressure p_c was large enough to inhibit any cavitation. This was accomplished by monitoring the total mean-square energy over the entire spectra for various values of σ. It was found that, for a constant discharge Q and valve opening b, the total energy did not vary if σ was above a certain threshold value, to be discussed later. The tests under non-cavitating conditions were also of value in observing changes in the jet flow pattern for different conditions.

The pressure transducers P_1 and P_2 in the model and P_1 in the prototype chamber experience the acoustical noise from the confined jet issuing from the annular orifice. The fact that the discharge coefficient is constant over the range of Reynolds numbers tested would suggest a turbulent jet. As shown by McCloy and Beck [8] in their study of jet hysteresis the jet can either reattach on the surface of the spool or on the wall of the port, or issue freely. A shifting jet pattern was clearly indicated in the model chamber by observing the energy levels on the two transducers, which were located at the extremities of the cavity.

The dynamics of an unconfined plane jet issuing from a nozzle are fairly well documented, albeit at higher Reynolds numbers than experienced with the two valves. As experimentally shown by Albertson et al [10], and later by Gutmark and Wygnanski [11], the mean centerline velocity of a plane jet decreases as the square root of the ratio of the initial jet diameter to the axial distance. In terms of the definition sketch on Fig. 5

$$\frac{V_j}{V_c} = K\sqrt{\frac{b}{\ell}} \qquad (10)$$

in which K is a constant for plane jets at large Reynolds number, and ℓ is the axial distance from the nozzle, or from the vena contracta in the case of an orifice. For a

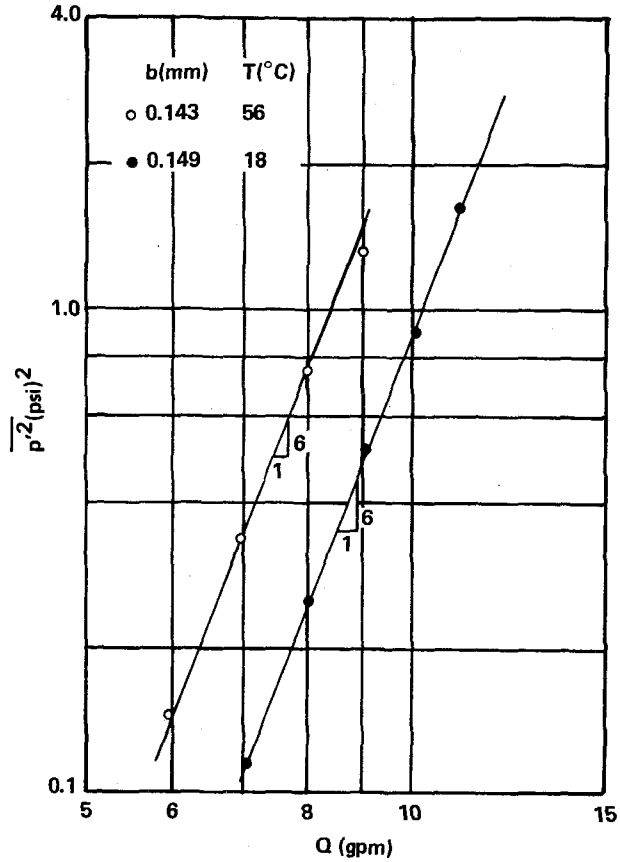

Fig. 6 Non-cavitating mean-square energy versus discharge for prototype valve at a fixed opening

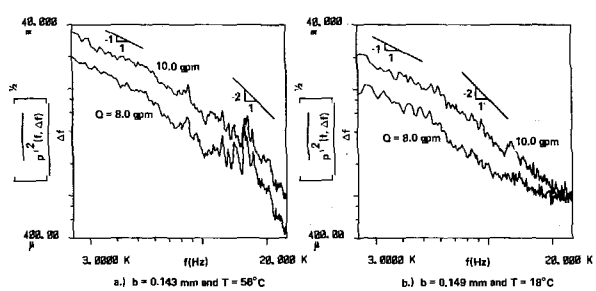

Fig. 7 Non-cavitating energy spectra for prototype valve at a fixed opening

plane turbulent jet Gutmark and Wygnanski [11] found that the r.m.s. value of the fluctuating velocity u'_o on the centerline of the jet was a constant when normalized with V_j, or

$$\frac{\sqrt{u_o'^2}}{V_j} = \text{constant} \qquad (11)$$

Reethof [12] states that a fluctuating mass flow rate with in-phase pressure

fluctuations would correspond to a monopole source, for which the r.m.s. energy of fluctuating pressure in this case is assumed to be correlated by

$$\sqrt{p'^2} = B_1 \rho V_j^2 \qquad (12)$$

in which B_1 is a dimensionless coefficient which would depend upon transducer location, Reynolds number, etc. If instead the fluctuations emanate from dipole sources -- which may be related directly to fluctuating pressures

$$\sqrt{p'^2} = B_2 \rho V_j^2 \left(\frac{V_j}{a}\right) \qquad (13)$$

in which a is the acoustic velocity. For a monopole source Eq. 12 along with the jet relationships (3, 4, 10) yield the mean-square energy

$$\overline{p'^2} = B_1^2 \left[\frac{K}{\pi C_c}\right]^4 \frac{\rho^2}{D^4 b^2 \ell^2} Q^4 \qquad (14)$$

In the case of dipole sources

$$\overline{p'^2} = B_2^2 \left[\frac{K}{\pi C_c}\right]^6 \frac{\rho^2 Q^6}{D^6 b^3 \ell^3 a^2} \qquad (15)$$

All non-cavitating spectra measured by transducer P_1 in the chamber of the prototype valve indicate that the mean-square energy can be correlated in terms of a dipole, or fluctuating pressure, source. The mean-square energies measured with this transducer correlate well with Q^6, as shown by the two data sets in Fig. 6. The data shown in Fig. 6 were taken at virtually the same opening b, but quite different Reynolds numbers. If ℓ is assumed to be fixed and to correspond to the distance from the orifice opening to transducer P_1, then Eq. 15 can be reduced to

$$\overline{p'^2} = B_3 \rho^2 Q^6 \qquad (16)$$

as a, D, and b are virtually constant. Although there is a Reynolds number variation for each data set the coefficient B_3 appears to be a constant for each. Energy spectra for two of the data points plotted on Fig. 6 are presented in Fig. 7. The slope of each curve can be approximated by -1 for the lower frequency range and -2 for the higher frequencies. As demonstrated by Lush [13] a dipole source will produce energy spectra with a -1 slope. As most of the energy is in the first half of the frequency range shown in Fig. 7, the dipole source dominates, resulting in a relationship represented by Eq. 15. An examination of many non-cavitating spectra shows that, as the flow rate and hence jet velocity V_j is increased for a fixed opening b, the extent of the spectrum corresponding to a -1 slope increases.

The two pressure transducers in the model were located such that any significant changes in the jet orientation could be noticed. The non-cavitating results presented here suggest that the jet did flip back and forth, confirming the conclusions of McCloy and Beck [8] that the jet may reattach to either the spool surface or the port wall, or issue freely at an angle depending upon the opening b and any clearance between the spool and the valve body.

The variation of mean-square energy with

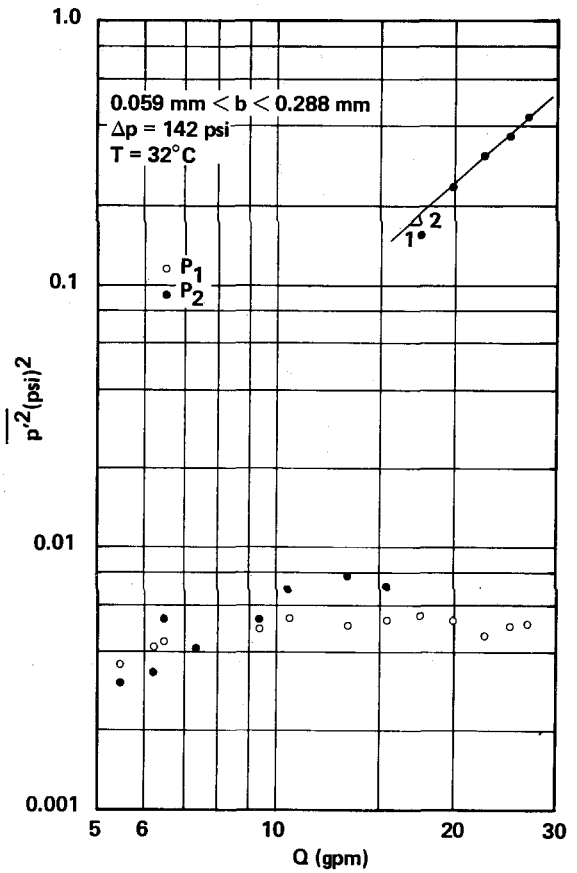

Fig. 8 Non-cavitating mean-square energy versus discharge for model valve at a variable opening and constant pressure difference

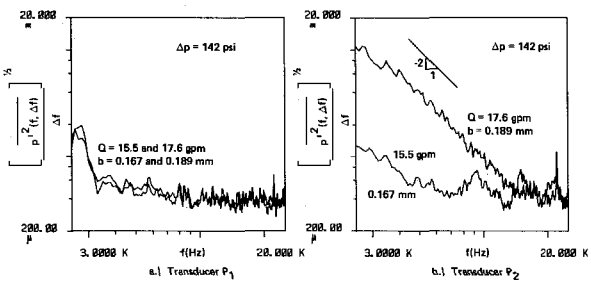

Fig. 9 Non-cavitating energy spectra for model valve at two values of opening b and constant pressure difference

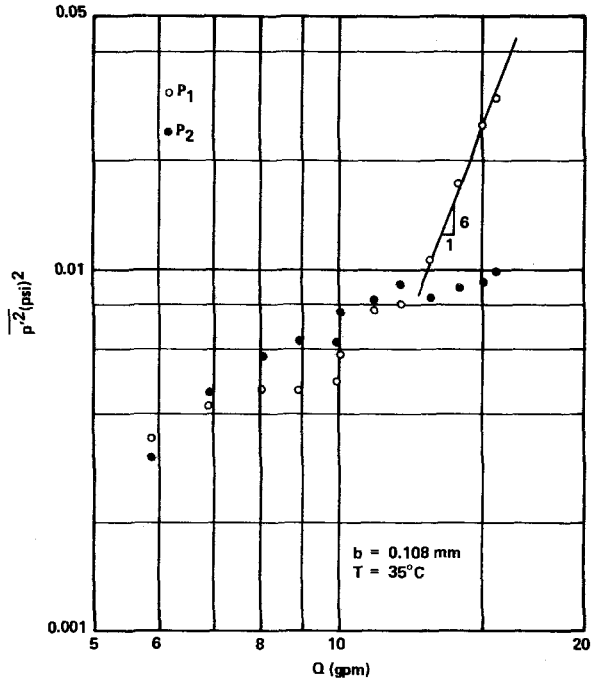

Fig. 10 Non-cavitating mean-square energy versus discharge for model valve at a fixed opening

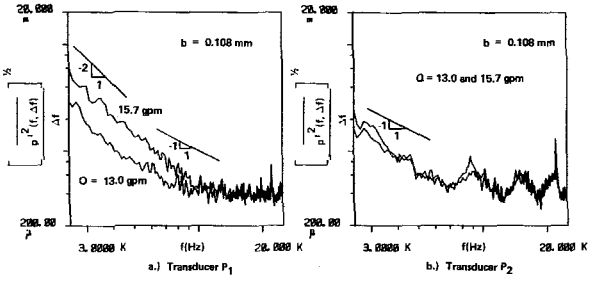

Fig. 11 Non-cavitating energy spectra for model valve at a fixed opening

flow rate is shown in Fig. 8 for various openings of the model valve. The pressure difference Δp was maintained constant under non-cavitating conditions. For a free jet for which Δp is a constant the velocity at the vena contracta V_c as given by Eq. 2 should have been a constant for all of the data shown in Fig. 8. According to Eq. 10 the jet velocity at some position ℓ from the vena contracta would increase directly with the square root of the opening b. The nearly constant output from transducer P_1 over the range of openings would indicate that the jet was not directed toward P_1. For flows less than 15.5 gpm the jet is probably between P_1 and P_2 because of the relatively low energy levels. As shown by Fig. 8 and the corresponding spectra in Fig. 9 for transducer P_2 there is

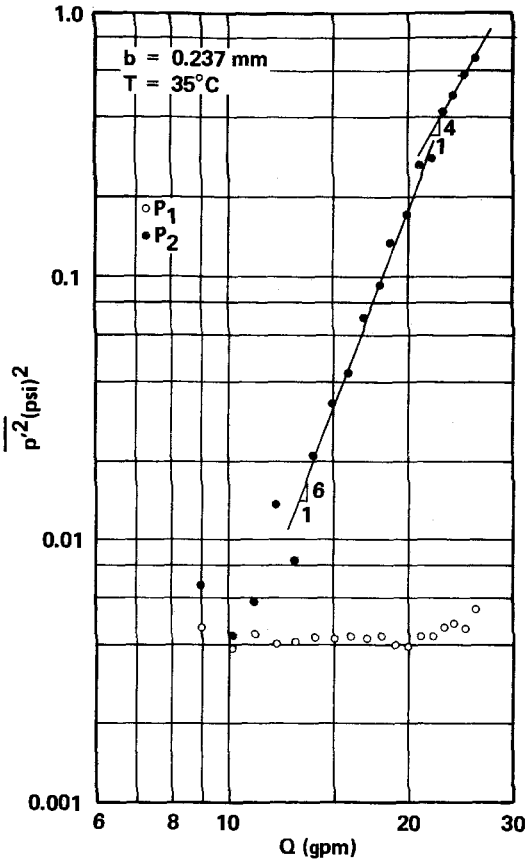

Fig. 12 Non-cavitating mean-square energy versus discharge for model valve at a fixed opening

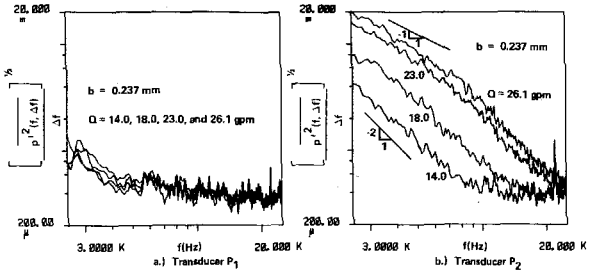

Fig. 13 Non-cavitating energy spectra for model valve at a fixed opening

an apparent shift in the flow pattern as the flow increased slightly from 15.5 to 17.6 gpm. As the valve is opened further the energy level sensed by P_2 increases as the square of the flow, suggesting a monopole source in accordance with Eqs. 5 and 14 for a variable opening b. It is suspected that the increase in energy is either due to direct impingement of a reattached jet or the nearly direct effect of a free jet. The slope of the energy spectra at location P_2 can be approximated by -2 over a range of frequencies.

Non-cavitating data were collected with

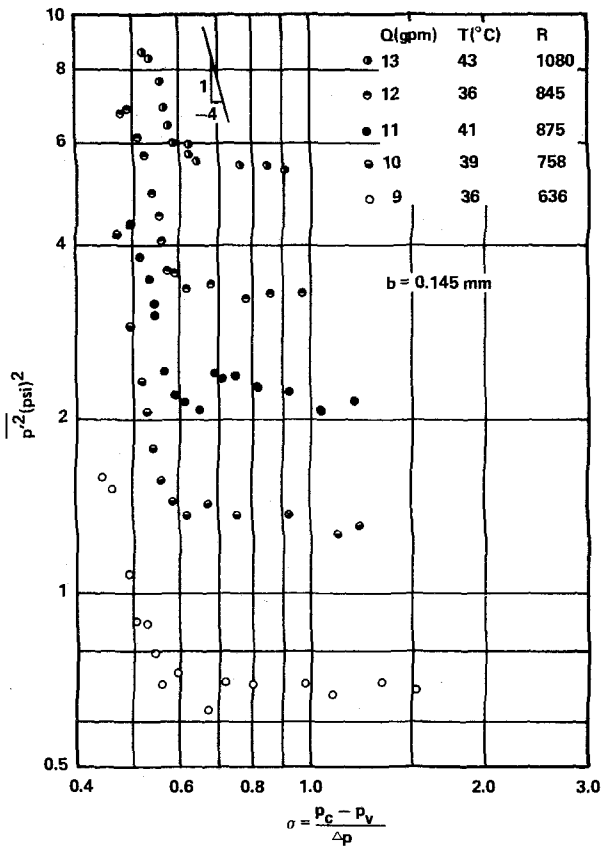

Fig. 14 Mean-square energy versus cavitation index for prototype valve at a fixed opening and constant discharges

the model valve fixed at openings of b = 0.108 and 0.237 mm. For the smaller opening the plot of mean-square energy versus flow rate shown in Fig. 10 and energy spectra for two of the higher flow rates plotted in Fig. 11 indicate that the jet may have been free, and furthermore directed toward transducer P_1. At the greater opening, however, the transducer P_1 hardly experienced any change in energy fluctuations as the flow increased, as shown in Figs. 12 and 13a. There is some indication that the slope of the mean-square energy versus flow rate correlation changes from a dipole source (6 to 1) to a monopole source (4 to 1) at the higher flow rates. Portions of the jet-induced spectra plotted in Fig. 13b can be approximated by slopes of -1, and others by -2.

The direct effect of pressure fluctuations from a jet are clearly shown in Figs. 9b, 11a, and 13b for the model, in contrast to Figs. 9a and 13a, for which there is little to no jet effect, but instead only background noise. The effect of any shifting of the jet is more evident in the larger model than in the prototype valve because of the size of the piezoelectric transducers relative to the length of the valve chamber.

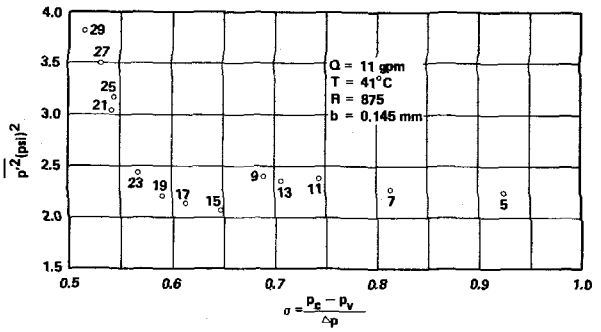

Fig. 15 Mean-square energy versus cavitation index for prototype valve at a fixed opening and Q = 11 gpm

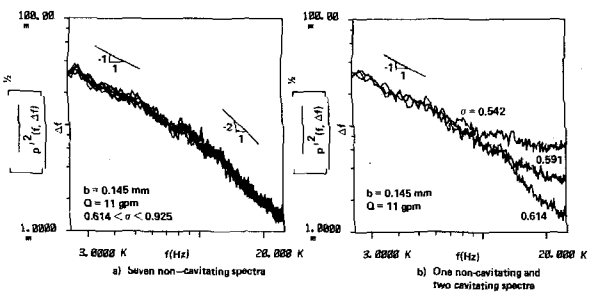

Fig. 16 Non-cavitating and cavitating energy spectra for prototype valve at a fixed opening and Q = 11 gpm

CAVITATING SPECTRA

In order to define and determine the condition of cavitation inception, tests were conducted over a range of values of the cavitation number σ. Because of the sensitivity of pressure fluctuations to changes in jet velocity, care was taken to maintain the volumetric flow Q constant and to hold the respective spool at a fixed position. As shown by the non-cavitating energy spectra slight differences in valve opening b can lead to significant changes in energy levels if there is a direct effect of the jet. On the other hand, however, cavitation noise in the model valve can be several orders of magnitude greater than that due to a non-cavitating jet.

Prototype Valve

The results of varying σ as b and Q are maintained nearly constant are presented in Fig. 14 for five flow rates. Although for each flow rate there is a sudden increase in the fluctuating energy measured by the pressure transducer P_1 as the chamber pressure p_c is lowered, it is not clear where cavitation inception occurs. The definition of incipient cavitation is especially difficult with the prototype valve because of the relatively large jet energy under non-cavitating conditions. In order to illustrate this difficulty the data points for Q = 11 gpm are replotted on Fig. 15 at a different scale. For reference each data point is given a number, which actually

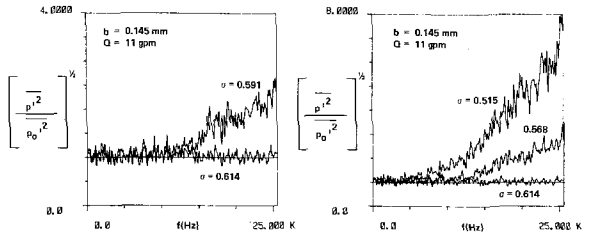

Fig. 17 Ratio of cavitating to non-cavitating (σ_o = 0.647) spectral density for prototype valve at a fixed opening

corresponds to a data file on a storage tape. The definition of cavitation inception would be very difficult if not impossible on the basis of mean-square energy, because of the sudden decrease in energy level from test 9 to test 15. It was discovered that an inspection of the respective energy spectra for each test proved more revealing than the total energy in the entire spectrum. In Fig. 16a the individual spectra for the seven points for which $\sigma > 0.6$ are superimposed, while the spectra for points 17, 19 and 21 are plotted in Fig. 16b. The coincidence of the data on Fig. 16a suggests only non-cavitating jet noise. Apparently few if no cavitation events occurred for σ = 0.614 (17), but many were present once the cavitation number was slightly reduced to 0.591 (19). Due to the relatively high energy levels at the low frequency end of the spectrum resulting from jet noise, small increases in the spectral density at the higher frequencies as a result of limited cavitation does not contribute much to the total energy over the entire spectrum. The parameter total energy becomes more indicative of cavitation levels once cavitation becomes more extensive.

The spectra in Fig. 16b indicate that cavitation noise is restricted to the higher frequencies, but extends over a wider band as the cavitation number decreases. Another measure of cavitation noise is the ratio of the power spectral density of each frequency channel Δf under cavitating conditions to that under non-cavitating conditions. Choosing test 15 (σ = 0.647) as the non-cavitating reference value, the ratio of power spectral densities are plotted in Fig. 17a for test 17 (σ = 0.614) and test 19 (σ = 0.591). Additional ratios of the power spectral density are presented in Fig. 17b for lower values of the cavitation index, showing a progressive expansion of the cavitation noise to lower frequencies as σ is decreased. A sensitive measure of the extent of cavitation noise is the area under the curve of the ratio of power spectral density versus frequency, as shown on Fig. 18 for Q = 12 gpm. Similar correlations occurred for five other flow rates.

Model Valve

The variation of mean-square energy versus the cavitation number is shown on Fig. 19

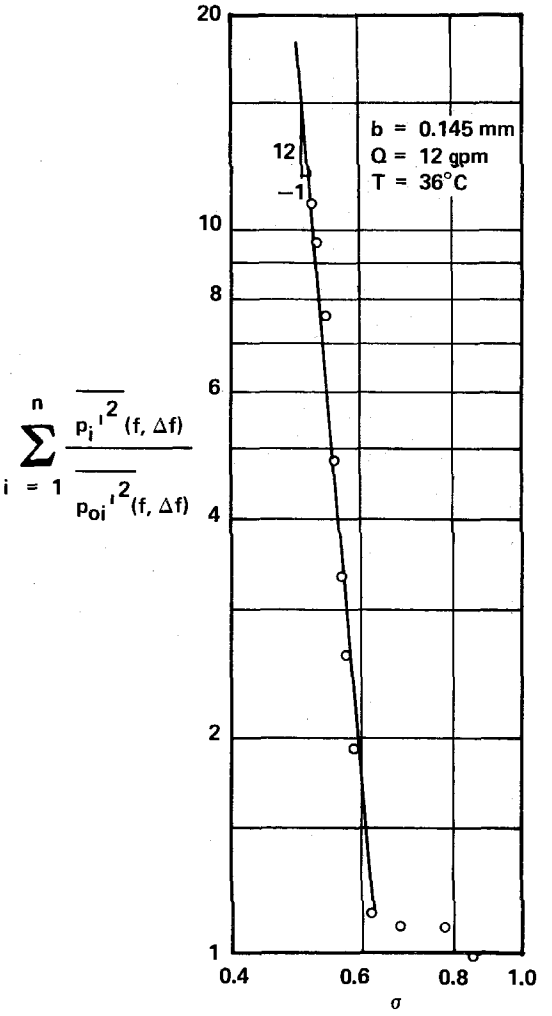

Fig. 18 Area under ratio of cavitating to non-cavitating mean-square spectral density curve versus cavitation index for prototype valve at a fixed opening

for two openings of the model valve. Selected spectra are plotted in Fig. 20 for the smaller opening (Q = 10 gpm), and in Fig. 21 for the larger opening (Q = 20 gpm).

For Q = 10 gpm there is only a limited effect of the jet under non-cavitating conditions, resulting in relatively low energy levels for the four pairs of data for P_1 and P_2 plotted on Fig. 19. Once σ was lowered to 0.269, however, the noise increased approximately tenfold on both transducers. In contrast to the results for the prototype valve cavitation noise in the model valve is evident over a wider band of frequencies. A further lowering of the cavitation number increased the energy level at least another order of magnitude, as shown by Fig. 19. From σ = 0.269 to σ = 0.189 the increase in noise is rather broadband, at least from 2.5 kHz < f < 25 kHz. Fig. 19 clearly demonstrates the dramatic sensitivity of the fluctuating pressure to the onset of cavitation events.

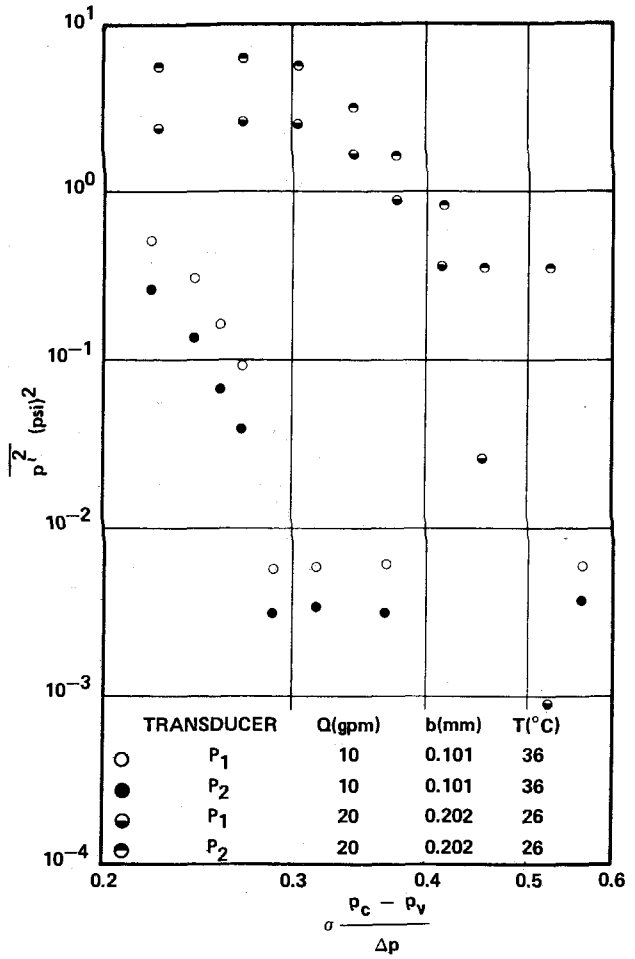

Fig. 19 Mean-square energy versus cavitation index for model valve at two fixed openings

At the greater valve opening the jet has a direct effect on transducer P_2, Fig. 21b, under both non-cavitating and cavitating conditions. The energy level measured by transducer P_1 under non-cavitating conditions (σ = 0.523 in Fig. 19) is quite low compared to that indicated by P_2. Transducer P_1 is much more sensitive to the onset of cavitation, however, because of the low background level under no cavitation. As the cavitation index was lowered from 0.523 through inception to a value of 0.452 the increase in noise measured by transducer P_1 was significantly greater than that sensed by transducer P_2. As the cavitation number was lowered further the noise as measured by transducer P_1 continued to increase over a wide band. This increase was not sensed by transducer P_2 at the low frequencies because of the intense background noise of the jet, which may have been directed upon P_2.

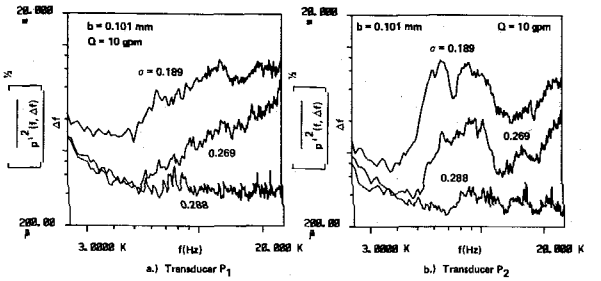

Fig. 20 One non-cavitating and two cavitating energy spectra for model valve at a fixed opening

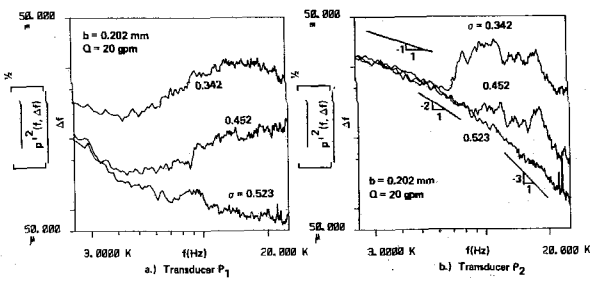

Fig. 21 One non-cavitating and two cavitating energy spectra for model valve at a fixed opening

CAVITATION INCEPTION

Attempts were made to formulate a criterion for the definition of incipient cavitation. Although the model was made of transparent walls for the purpose of visualization of the formation and collapse of bubbles, and the bubbles could be clearly seen as the valve was made to cavitate somewhat extensively, the onset of cavitation was extremely difficult to define visually because of the small openings, high jet velocities, and relatively small bubbles. After a number of somewhat unsuccessful attempts to establish incipient and desinent cavitation visually, reliance was placed upon the pressure transducers and the accelerometer, as well as aural sensing using a stethoscope. The identification of inception was much easier in the model using transducer P_1 because of the dramatic change once cavitation commences. Because of the difficulty of separating jet noise from cavitation noise the criterion for inception used for the prototype valve differed slightly from that applied to the model valve, the latter of which will be discussed first.

Model Valve

Because of the relatively low levels of energy in the model under non-cavitating conditions, except when the jet was apparently directed onto transducer P_2, it was not difficult to observe the occurrence of a few

cavitation events by comparing cavitating with non-cavitating spectra. The data were taken by maintaining a constant flow with the spool locked in a fixed position. The cavitation number was reduced as the pressure difference Δp, and consequently the discharge Q, was maintained constant as nearly as possible. For each value of σ the dynamic signal for transducer P_1 was processed and the total fluctuating energy noted. It was observed that this value hardly changed under non-cavitating conditions. Cavitation inception was defined at the condition for which this nominal value increased by approximately 50 to 100 percent, which corresponded to only the slightest change in the cavitation index. Usually aural sensing by means of a stethoscope yielded the same value of the critical cavitation number. The cavitation number at the 50 to 100 percent energy increase is defined as the incipient cavitation index σ_i, and is plotted as a function of the Reynolds number in Fig. 22. The two sets of data correspond to a range of flow rates for each value of the fixed opening b.

Prototype Valve

As mentioned earlier a comparison of fluctuating energies measured by the pressure transducer in the chamber of the prototype valve did not clearly indicate the difference between cavitation inception or limited cavitation and no cavitation because of the high level of jet noise. The points shown on Fig. 15 for $\sigma > 0.6$ illustrate the difficulty inherent with comparing solely mean-square energy, while the spectra on Fig. 16a suggest there is no cavitation. Only by comparing spectra, Fig. 16b, or normalizing the spectral density with the corresponding non-cavitating spectra, Fig. 17, could the presence of cavitation be determined. The criterion for incipient cavitation for the prototype valve was defined as the departure of the area under the normalized spectral density curves versus cavitation number from the non-cavitating value, which usually varied from approximately 0.9 to 1.1, depending upon which non-cavitating test was chosen as the reference value. The value of σ_i was obtained from expanded versions of Fig. 18 by interpolating between the intersection of the extrapolated curve on the cavitating leg of the plot and the non-cavitating horizontal line. Various criteria yielded differences in the incipient cavitation number of only 0.005 to 0.01. The results of two series of tests at virtually the identical valve opening and nearly the same range of flow rates (7-13 gpm) are shown in Fig. 22. The only difference in the two series was the oil temperature, which resulted in a significant difference in the range of Reynolds numbers.

DISCUSSION OF RESULTS

The criteria of cavitation inception employed in this investigation corresponds to a few, but unknown number, of cavitation events during the 50 ensemble averages taken over the sampling period. Single bubble formation in the transparent model could not be observed under these conditions. In fact, the

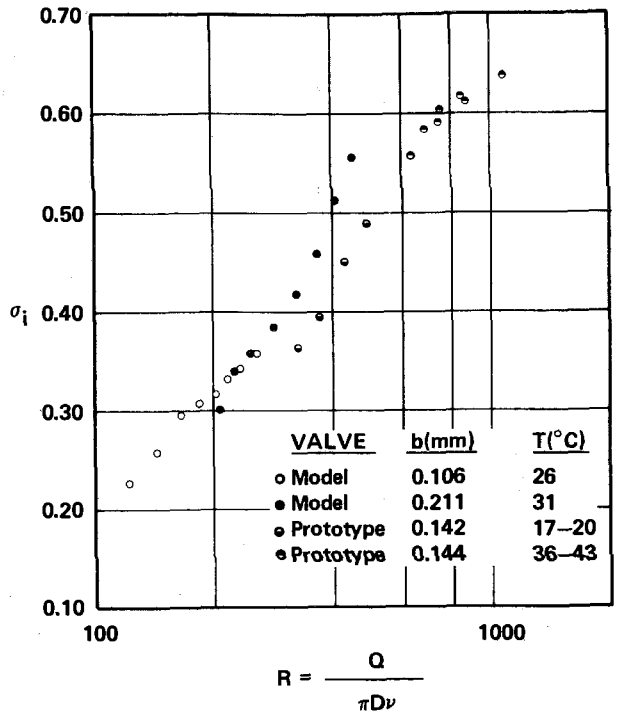

Fig. 22 Incipient cavitation index versus Reynolds number for model and prototype valves

cavitation index corresponding to the formation of a series of bubbles around the annulus was approximately 0.18 less than the values shown on Fig. 22. Even a desinent cavitation number defined at the condition of the elimination of all visible bubbles was 0.10 smaller than the corresponding values of σ_i depicted on Fig. 22. Because of the smallness of the bubbles, the high jet velocity, and the apparently few cavitation events, bubbles at the condition σ_i are difficult to observe.

For the range of values of dissolved air content present in this study there was no apparent effect of hysteresis on σ_i. The critical σ_i did not appear to depend upon whether the downstream pressure was being decreased or increased. For dissolved air content at the two extremes experienced in the investigation -- 4.5 and 9.0 percent -- there was no apparent difference in σ_i nor cavitation noise over the entire range of the cavitation index. Evidently the low residence time of the bubbles in the jet and valve chamber precluded any significant effect of gaseous cavitation. Even for the lowest values of the cavitation number experienced by the model valve, the bubbles disappeared as the flow left the downstream port, suggesting the presence of only vaporous cavitation.

Although the accelerometer mounted on the end of the spool of the prototype valve was not quite as sensitive to the onset of cavitation, it proved to be quite a good indicator of the level of cavitation once inception occurred. As the cavitation index was lowered toward σ_i, as represented by Fig. 14, there was a very gradual increase in the fluctuating

acceleration levels, making the formulation of a criterion of cavitation inception on the basis of the accelerometer quite difficult. The low level response on the accelerometer for $\sigma > \sigma_i$ is attributed to mechanical effects caused by the method utilized to vary σ -- the operation of downstream valves.

No attempt was made to measure the size of free nuclei in the oil, although the high pressure filter limited the absolute size of any contaminant to 3 μm. Because of the continual filtering of the test liquid the nuclei size and distribution probably did not vary much from test to test, as was evident from a comparison of energy spectra from test series to test series at the same conditions. As shown by the data on Fig. 6 for two different temperatures there is an apparent viscous effect on the non-cavitating energy spectra. Since cavitation inception is affected by the level of turbulence, as shown by Arndt [14,15], the variation of σ_i with Reynolds number shown in Fig. 22 can be directly correlated with the non-cavitating fluctuating energy shown in Fig. 6. The data of McCloy and Beck [3] indicate a similar trend of σ_i versus R for two two-dimensional models. Their incipient cavitation index was based on the aural detection of the initial presence of a sharp crackling sound. For the range of Reynolds numbers the critical values of σ_i reported by McCloy and Beck [3] are 0.05 to 0.10 lower than the corresponding ones plotted on Fig.22, however. Perhaps the criterion employed in this investigation corresponds to a smaller number of cavitation events at σ_i. The effect of viscosity on cavitation inception is also evident in the results of Backé and Riedel [5] and Riedel [6], who evidently defined inception at the condition of the change in the discharge coefficient of an orifice, or a situation corresponding to wider spread cavitation. Noise data taken by Rouse [16] with a water jet issuing from a nozzle yielded $\sigma_i = 0.55$ from a plot of noise versus σ. Intermittent bursts of noise were observed for values of σ as high as 0.7, however. Obviously, the criterion employed for cavitation inception is somewhat subjective.

CONCLUSIONS

Changes in flow pattern and jet orientation in the chamber of spool valves can be sensed by high-frequency response pressure transducers strategically placed. Under non-cavitating conditions jet noise can frequently be directly correlated with the valve opening and flow rate. For the Reynolds numbers tested in this study there is a definite effect of viscosity on pressure fluctuations emanating from a turbulent non-cavitating jet.

The effect of dissolved gas content on cavitation in spool valves is minimal if the gas content does not exceed that corresponding to atmospheric conditions.

High-frequency response pressure transducers are good diagnostic tools for detection of cavitation inception and cavitation intensity, while a high-frequency response accelerometer is a sensitive indicator of noise levels under cavitating conditions.

The ratio of cavitation noise to non-cavitating noise is greater at higher frequencies than at lower frequencies, especially if there is a direct influence of jet noise.

Cavitation inception can be identified most easily by (a) comparison of auto power spectra and (b) ratio of cavitating spectra to non-cavitating spectra for the same test conditions.

For the range of data presented in this paper the critical cavitation number is a function of the Reynolds number.

ACKNOWLEDGMENTS

This investigation was supported in full by the Air Force Base Propulsion Laboratory through AFOSR Contract F33615-77-C-2036, which was administered by Project Engineer Paul D. Lindquist. The authors would also like to acknowledge the direct contribution of J. I. Craig, F. D. Lewis and H. J. Bates.

REFERENCES

1 McCloy, D. and Martin, H. R., The Control of Fluid Power, Longman, London, 1973.

2 MacLellan, M. A., Mitchell, A. E. and Turnbull, D. E., "Flow Characteristics of Piston-Type Control Valves," Proceedings of the Symposium on Recent Mechanical Engineering Developments in Automatic Control, Institution Mechanical Engineers, London, Jan. 1960, pp. 13-30.

3 McCloy, D. and Beck, A., "Some Cavitation Effects in Spool Valve Orifices," Proceedings Institution Mechanical Engineers, Vol. 182, Pt. I, No. 8, 1967-68, pp. 163-174.

4 Backé, W. and Benning, P., "Über Kavitationserscheinungen in Querschnittsverengungen von ölhydraulischen Systemen," Industrie-Anzeiger, Vol. 63, 1962, pp. 35-42.

5 Backé, W. and Riedel, H.-P., "Kavitation in ölhydraulischen Systemen," Industrie-Anzeiger, Vol. 94, 1972, pp. 153-158.

6 Riedel, H.-P., "Kavitationsverhalten von verschiedenen Druckflüssigkeiten," Industrie-Anzeiger, Vol. 94, 1972, pp. 1724-1727.

7 Lichtarowicz, A. and Pearce, I. D., "Cavitation and Aeration Effects in Long Orifices," Cavitation Conference, Institution Mechanical Engineers, Edinburgh, 1974.

8 McCloy, D. and Beck, A., "Flow Hysteresis in Spool Valves," Proceedings of the First BHRA Fluid Power Symposium, Cranfield, 1969, pp. 170-182.

9 Robertson, J. M., Hydrodynamics in Theory and Application, Prentice-Hall, New York, 1965.

10 Albertson, M. L., Dai, Y. B., Jensen, R. A. and Rouse, H., "Diffusion of Submerged Jets," Transactions, ASCE, Vol. 115, 1950, pp. 639-664.

11 Gutmark, E. and Wygnanski, I., "The Planar Turbulent Jet," Journal of Fluid Mechanics, Vol. 73, 1976, pp. 465-495.

12 Reethof, G., "Turbulence - Generated Noise in Pipe Flow," Annual Review of Fluid Mechanics, Vol. 10, 1978, pp. 333-367.

13 Lush, P. A., "Measurements of Subsonic Jet Noise and Comparison with Theory," Journal

of Fluid Mechanics, Vol. 46, 1971, pp. 477-500.

14 Arndt, R. E. A., "Pressure Fields and Cavitation," Proceedings of the 7th IAHR Symposium on Hydraulic Machinery, Vienna, 1974, Paper IX.

15 Arndt, R. E. A., "Investigation of the Effects of Dissolved Gas and Free Nuclei on Cavitation and Noise in the Wake of a Sharp Edged Disk," Proceedings of Joint ASME-IAHR-ASCE Symposium on Hydraulic Machinery, Fort Collins, Colorado, 1978, pp. 543-556.

16 Rouse, H., "Cavitation in the Mixing Zone of a Submerged Jet," La Houille Blanche, Vol. 8, No. 1, 1953, pp. 9-19.